

# Phonon effects on the radiative recombination of excitons in double quantum dots

Paweł Karwat, Anna Sitek, and Paweł Machnikowski\*  
*Institute of Physics, Wrocław University of Technology, 50-370 Wrocław, Poland*

We study theoretically the radiative recombination of excitons in double quantum dots in the presence of carrier-phonon coupling. We show that the phonon-induced pure dephasing effects and transitions between the exciton states strongly modify the spontaneous emission process and make it sensitive to temperature, which may lead to non-monotonic temperature dependence of the time-resolved luminescence. We show also that under specific resonance conditions the biexcitonic interband polarization can be coherently transferred to the excitonic one, leading to an extended life time of the total coherent polarization, which is reflected in the nonlinear optical spectrum of the system. We study the stability of this effect against phonon-induced decoherence.

PACS numbers: 78.67.Hc, 78.47.jd, 71.38.-k, 03.65.Yz

## I. INTRODUCTION

Systems composed of coupled nanostructures attract much attention as they not only open the path to new applications but also provide new ways of controlling the states and dynamics of confined carriers. For instance, systems build of two closely located quantum dots provide the basis for an implementation of excitonic qubits with extended life times<sup>1</sup>, allow one to effect conditional quantum control of carrier states<sup>2</sup>, and have been proposed as a source of entangled photons<sup>3</sup>. Carrier transfer in such double quantum dot (DQD) structures can also be used for initializing the spin state of a dopant Mn atom in one of the dots<sup>4</sup>.

The optical properties of the DQD structures are much more complex than those of a single quantum dot (QD), which is manifested in the occupation and coherence dynamics observed in optical experiments<sup>5-7</sup>. This is partly due to the richer structure of carrier states<sup>8-11</sup> but also to the interplay of a few other factors that govern the evolution of carriers in these systems after an optical excitation: collective spontaneous emission (radiative recombination of excitons)<sup>12</sup>, coupling between the dots<sup>13</sup>, as well as phonon-induced transitions<sup>14-17</sup> and dephasing<sup>18-20</sup>. In our previous work, we have investigated the effect of the first two of these factors<sup>12</sup> and their role in the linear<sup>21</sup> and nonlinear<sup>22</sup> response of DQDs. We have shown, in particular, that collective effects in the spontaneous emission of uncoupled DQDs disappear as soon as the transition energy mismatch between the dots forming the system exceeds the spectral line width of the fundamental transition (on the order of micro-electron-Volts), which is well beyond current manufacturing possibilities. However, coupling between the dots leads to pronounced collective effects even for technologically realistic values of the energy mismatch on the order of milli-electron-Volts. We have also pointed out that phonon-related effects can affect the collective spontaneous emission in these systems<sup>23,24</sup>.

In this paper, we study the effects of phonon-induced transitions and dephasing on the kinetics of collective radiative recombination in DQDs. The interplay of these

two factors has recently been shown to determine the recombination properties of a lateral DQD system with direct to indirect exciton tunneling<sup>25</sup>. Here, we consider a vertically stacked system with realistic values of the parameters and focus on the experimentally observable features in the system dynamics assuming the spatially direct nature of the excitons (no electric field applied). We study the decay of the exciton occupation in a DQD in the presence of phonons and show that it becomes strongly dependent on temperature due to phonon-induced thermalization of single-exciton occupations and pure dephasing processes. For negative coupling (characteristic of tunneling), this leads to an increase of the exciton lifetime with temperature and to its non-monotonic behavior in a typical situation when thermally activated non-radiative decay processes are present at higher temperatures. We show also that for specific values of the system parameters, coherent transfer of interband polarization between the biexciton and exciton transitions can take place, which is reflected in the nonlinear optical spectroscopy of these systems, and we study the stability of this process against phonon-induced decoherence.

The paper is organized as follows. In Sec. II, we define the model under study. Next, in Sec. III, we define the method of numerical simulations and present a preliminary discussion of the most important phenomena that will determine the evolution, based on analytical solutions in the limiting cases. Sec. IV contains the results of our modeling and their discussion. Finally, Sec. V concludes the paper.

## II. MODEL

We consider a self-assembled structure composed of two vertically stacked QDs with relatively similar sizes in the absence of an external electric field. The lowest sector of exciton eigenstates is then formed by spatially direct states, that is, configurations in which the electron-hole pairs reside in the same dot<sup>11,26</sup>. We restrict the discussion to the lowest exciton state in each dot and assume that the spins of the carriers are fixed, corresponding to

bright exciton configurations. Under these assumptions, each dot can be either empty or occupied by one exciton and the model includes four basis exciton states: the state without excitons,  $|0\rangle$ , the states  $|1\rangle$  and  $|2\rangle$  with an exciton in the first and second dot, respectively, and the ‘‘molecular biexciton’’ state  $|B\rangle$  with excitons in both dots. The carriers confined in the QDs interact with the longitudinal acoustic phonon modes via the deformation potential coupling and with the photon (radiative) environment via the dipole coupling.

The total Hamiltonian of the system is

$$H = H_{\text{DQD}} + H_{\text{ph}} + H_{\text{rad}} + H_{\text{c-ph}} + H_{\text{c-rad}}.$$

The first term describes exciton states in the DQD structure and has the form

$$H_{\text{DQD}}^{(\text{S})} = \sum_{i=1,2} \epsilon_i |i\rangle\langle i| + (\epsilon_1 + \epsilon_2 + E_{\text{B}}) |B\rangle\langle B| + V(|1\rangle\langle 2| + |2\rangle\langle 1|), \quad (1)$$

where  $\epsilon_1$  and  $\epsilon_2$  are the fundamental excitonic transition energies in the two dots,  $V$  is the coupling between the dots, which may originate either from the Coulomb (Förster) interaction or from tunnel coupling (it can be assumed real),  $E_{\text{B}}$  is the biexciton shift, and the superscript ‘‘S’’ denotes the Schrödinger picture. Electron and hole wave functions in the dots 1 and 2 are modeled by identical anisotropic Gaussians with identical extensions  $l$  in the  $xy$  plane and  $l_z$  along the growth axis  $z$  for both particles,

$$\psi_{1,2}(\mathbf{r}) \sim \exp \left[ -\frac{x^2 + y^2}{2l^2} - \frac{(z \pm D/2)^2}{2l_z^2} \right], \quad (2)$$

where the upper (lower) sign refers to  $\psi_1$  ( $\psi_2$ ) and  $D$  is the distance between the dots.

The phonon modes are described by the free phonon Hamiltonian

$$H_{\text{ph}} = \sum_{\mathbf{k}} \hbar \omega_{\mathbf{k}} b_{\mathbf{k}}^\dagger b_{\mathbf{k}},$$

where  $b_{\mathbf{k}}, b_{\mathbf{k}}^\dagger$  are the bosonic operators of the phonon modes and  $\omega_{\mathbf{k}}$  are the corresponding frequencies. We assume a linear dispersion relation for phonons. Interaction of carriers confined in the DQD with phonons is modeled by the independent boson Hamiltonian

$$H_{\text{c-ph}} = \sum_{i=1,2} (|i\rangle\langle i| + |B\rangle\langle B|) \sum_{\mathbf{k}} f_{\mathbf{k}}^{(i)} (b_{\mathbf{k}}^\dagger + b_{-\mathbf{k}}), \quad (3)$$

where  $f_{\mathbf{k}}^{(1,2)}$  are system-reservoir coupling constants. For Gaussian wave functions as in Eq. (2), the coupling constants for the deformation potential coupling between confined charges and longitudinal phonon modes have the form  $f_{\mathbf{k}}^{(1,2)} = f_{\mathbf{k}} e^{\pm i k_z D/2}$ , where

$$f_{\mathbf{k}} = (\sigma_e - \sigma_h) \sqrt{\frac{k}{2\rho v c}} \exp \left[ -\frac{l_z^2 k_z^2 + l^2 k_{\perp}^2}{4} \right].$$

Here  $v$  is the normalization volume,  $k_{\perp}/z$  are momentum components in the  $xy$  plane and along the  $z$  axis,  $\sigma_{e/h}$  are deformation potential constants for electrons/holes,  $c$  is the speed of longitudinal sound, and  $\rho$  is the crystal density. We assume that off-diagonal carrier-phonon couplings are negligible due to small overlap of the wave functions confined in different dots.

The third component in our modeling is the radiative reservoir (modes of the electromagnetic field), described by the Hamiltonian

$$H_{\text{rad}} = \sum_{\mathbf{k}, \lambda} \hbar \omega_{\mathbf{k}} a_{\mathbf{k}, \lambda}^\dagger a_{\mathbf{k}, \lambda},$$

where  $a_{\mathbf{k}, \lambda}, a_{\mathbf{k}, \lambda}^\dagger$  are photon creation and annihilation operators and  $\omega_{\mathbf{k}}$  are the corresponding frequencies ( $\lambda$  denotes polarizations). The QDs are separated by a distance much smaller than the resonant wavelength so that the spatial dependence of the EM field may be neglected (the Dicke limit). The Hamiltonian describing the interaction of carriers with the EM modes in the dipole and rotating wave approximations is

$$H_{\text{c-rad}} = \Sigma_- \sum_{\mathbf{k}, \lambda} g_{\mathbf{k}, \lambda} a_{\mathbf{k}, \lambda}^\dagger + \text{H.c.}, \quad (4)$$

with

$$\Sigma_- = |0\rangle\langle 1| + |2\rangle\langle B| + |0\rangle\langle 2| + |1\rangle\langle B|$$

and

$$g_{\mathbf{k}, \lambda} = i \mathbf{d} \cdot \hat{e}_\lambda(\mathbf{k}) \sqrt{\frac{\hbar \omega_{\mathbf{k}}}{2 \epsilon_0 \epsilon_r v}},$$

where  $\mathbf{d}$  is the interband dipole moment,  $\epsilon_0$  is the vacuum permittivity,  $\epsilon_r$  is the dielectric constant of the semiconductor and  $\hat{e}_\lambda(\mathbf{k})$  is the unit polarization vector of the photon mode with the wave vector  $\mathbf{k}$  and polarization  $\lambda$ . For wide-gap semiconductors with the band gap on the order of an electron-Volt, zero-temperature approximation may be used for the radiation reservoir at any reasonable temperature.

In our numerical simulations (to be presented in Sec. IV), we take the parameters corresponding to a self-assembled InAs/GaAs system:  $\sigma_e - \sigma_h = 9$  eV,  $\rho = 5350$  kg/m<sup>3</sup>,  $c = 5150$  m/s, the wave function parameters  $l = 4.5$  nm,  $l_z = 1$  nm,  $D = 6$  nm, and the radiative recombination time (for a single dot)  $1/\Gamma_0 = 800$  ps.

### III. EVOLUTION

The evolution of the DQD density matrix in the interaction picture is given by the equation

$$\dot{\rho} = \mathcal{L}_{\text{rad}}[\rho] + \mathcal{L}_{\text{ph}}[\rho], \quad (5)$$

where  $\rho$  is the density matrix of the exciton subsystem and the two terms on the right-hand side account for the

radiative and phonon-induced dissipation and dephasing effects. Eq. (5) is valid in the leading order in both the couplings, where the two dissipation channels are additive.

The interaction of carries with the radiation reservoir leads to a Markovian evolution which can be described by a Lindblad generator. For a double dot, the analysis based on the Weisskopf–Wigner procedure<sup>12</sup> shows that the correct general description of the collective spontaneous emission is provided by the equation

$$\dot{\rho}^{(R)} = -\frac{i}{\hbar} \left[ H_{\text{DQD}}^{(R)}, \rho^{(R)} \right] + \mathcal{L}_{\text{rad}}^{(R)}[\rho^{(R)}],$$

where

$$\mathcal{L}_{\text{rad}}^{(R)}[\rho] = \Gamma_0 \left[ \Sigma_- \rho \Sigma_+ - \frac{1}{2} \{ \Sigma_+ \Sigma_-, \rho \}_+ \right].$$

Here the superscript ‘‘R’’ denotes the ‘‘rotating frame’’ picture defined by the unitary transformation  $e^{iS(t)}$ , with

$$S(t) = \frac{E}{\hbar} t (|1\rangle\langle 1| + |2\rangle\langle 2| + 2|B\rangle\langle B|),$$

where  $E = (\epsilon_1 + \epsilon_2)/2$ . That is,

$$\rho^{(R)} = e^{iS(t)} \rho^{(S)} e^{-iS(t)},$$

where  $\rho^{(S)}$  denotes the density matrix in the Schrödinger picture, and

$$\begin{aligned} H_{\text{DQD}}^{(R)} &= e^{iS(t)} H_{\text{DQD}}^{(S)} e^{-iS(t)} - \hbar \dot{S} \\ &= \Delta (|1\rangle\langle 1| - |2\rangle\langle 2|) + V (|1\rangle\langle 2| + |2\rangle\langle 1|) \\ &\quad + E_B |B\rangle\langle B|, \end{aligned} \quad (6)$$

where  $\Delta = (\epsilon_1 - \epsilon_2)/2$  is the parameter describing the transition energy mismatch between the dots. Since  $[S(t), H_{\text{DQD}}] = 0$  the density matrix in the interaction picture with respect to  $H_{\text{DQD}}$  is given by

$$\rho = e^{iH_{\text{DQD}}^{(R)} t/\hbar} \rho^{(R)} e^{-iH_{\text{DQD}}^{(R)} t/\hbar}$$

and the generator of the dissipative evolution becomes

$$\mathcal{L}_{\text{rad}}[\rho] = \Gamma_0 \left[ \Sigma_-(t) \rho \Sigma_+(t) - \frac{1}{2} \{ \Sigma_+(t) \Sigma_-(t), \rho \}_+ \right], \quad (7)$$

where  $\Sigma_-(t) = \Sigma_+^\dagger(t) = e^{iH_{\text{DQD}}^{(R)} t/\hbar} \Sigma_- e^{-iH_{\text{DQD}}^{(R)} t/\hbar}$  and  $\Gamma_0 = E^3 |\mathbf{d}|^2 \sqrt{\epsilon_r} / (3\pi\epsilon_0 c^3 \hbar^4)$  is the spontaneous decay rate for a single dot.

For the carrier-phonon interaction, non-Markovian effects can be important in some cases. Moreover, there seems to be no universal way to extract the Markov limit in various physical situations. Therefore, for the description of phonon-related effects, we use the time-convolutionless equation in the lowest order<sup>27</sup>

$$\mathcal{L}_{\text{ph}}[\rho] = - \int_0^t d\tau \text{Tr}_{\text{ph}} [H_{c-\text{ph}}(t), [H_{c-\text{ph}}(\tau), \rho(t) \otimes \rho_{\text{ph}}]], \quad (8)$$

where

$$H_{c-\text{ph}}(t) = e^{i(H_{\text{DQD}}^{(R)} + H_{\text{ph}})t/\hbar} H_{c-\text{ph}} e^{-i(H_{\text{DQD}}^{(R)} + H_{\text{ph}})t/\hbar}$$

is the carrier-phonon interaction Hamiltonian in the interaction picture,  $\rho_{\text{ph}}$  is the phonon density matrix at the thermal equilibrium, and  $\text{Tr}_{\text{ph}}$  denotes partial trace with respect to phonon degrees of freedom. Note that the form of  $H_{c-\text{ph}}$  is the same in the interaction and rotating frame pictures as  $[H_{c-\text{ph}}, S(t)] = 0$ .

The states  $|0\rangle$  and  $|B\rangle$  are eigenstates of the DQD Hamiltonian, therefore nontrivial evolution generated by  $H_{\text{DQD}}^{(R)}$  takes place only in the subspace spanned by  $|1\rangle, |2\rangle$ . From the point of view of the theoretical analysis, it is convenient to introduce the parametrization  $\Delta = \mathcal{E} \cos \theta$ ,  $V = \mathcal{E} \sin \theta$ , with  $\mathcal{E} > 0$  and  $\theta \in [-\pi, \pi)$ , and to treat  $\mathcal{E}$  and  $\theta$  as the independent parameters of the model. Then, the single-exciton eigenstates of the excitonic Hamiltonian can be written as

$$\begin{aligned} |+\rangle &= \cos \frac{\theta}{2} |1\rangle + \sin \frac{\theta}{2} |2\rangle, \\ |-\rangle &= -\sin \frac{\theta}{2} |1\rangle + \cos \frac{\theta}{2} |2\rangle, \end{aligned}$$

and correspond to the energies  $\pm \mathcal{E}$ . Thus,  $2\mathcal{E}$  is the energy splitting between the single-exciton eigenstates of  $H_{\text{DQD}}^{(R)}$  and  $\theta$  is the mixing angle of the single-exciton states.

The evolution equation (5) can be solved numerically at moderate computational cost<sup>23</sup>. However, some physical insight is gained if the two evolution generators given by Eq. (7) and Eq. (8) are treated to some extent analytically.

For the spontaneous emission, we expand the generator (7) in terms of the eigenstates of  $H_{\text{DQD}}^{(R)}$ . In the present discussion we assume that both the energy splitting parameter  $\mathcal{E}$  and the biexciton shift  $E_B$  are much larger than the inverse recombination time. This is reasonable as the energy mismatch and the coupling are typically on the order of milli-electron-Volts, while the recombination time is  $\tau_R \sim 1$  ns, yielding  $\hbar/\tau_R \sim 1$   $\mu\text{eV}$ . Then, we can neglect the oscillating terms proportional to  $e^{\pm i\mathcal{E}t/\hbar}$  and  $e^{\pm iE_B t/\hbar}$ . This leads to the emission-induced evolution of the exciton and biexciton occupations given (in the interaction picture) by

$$\dot{\rho}_{\pm\pm} = \Gamma_{\pm} (\rho_{BB} - \rho_{\pm\pm}), \quad \dot{\rho}_{BB} = -2\Gamma_0 \rho_{BB}, \quad (9a)$$

where  $\rho_{\alpha\beta} = \langle \alpha | \rho | \beta \rangle$  and  $\Gamma_{\pm} = \Gamma_0 (1 \pm \sin \theta)$ . The optically active coherences (optical polarizations) corresponding to the exciton and biexciton transitions evolve according to

$$\dot{\rho}_{0\pm} = -\frac{1}{2} \Gamma_{\pm} \rho_{0\pm} + \Gamma_{\pm} \rho_{\pm B} e^{i(E_B \mp 2\mathcal{E})t/\hbar}, \quad (9b)$$

$$\dot{\rho}_{\pm B} = -(\Gamma_0 + \Gamma_{\pm}/2) \rho_{\pm B}, \quad (9c)$$

while the evolution of the ‘‘dark’’ exciton-exciton and vacuum-biexciton coherences is described by

$$\dot{\rho}_{0B} = -\Gamma_0 \rho_{0B}, \quad \dot{\rho}_{\pm\mp} = -\Gamma_0 \rho_{\pm\mp}. \quad (9d)$$

One of the two essential effects following from Eqs. (9a)-(9d) is the appearance of the two different decay rates  $\Gamma_{\pm}$ . As a consequence, one of the single-exciton states is brighter (decays faster) and the other one is darker (decays slower) than a single exciton state in an individual dot (from now on, the terms “dark” and “bright” will always refer to the spatial state in the DQD structure; the spin configuration is always assumed to correspond to a bright exciton). For  $\theta = \pm\pi/2$ , one recovers the perfect superradiance (doubled decay rate) and subradiance (no radiative decay) of the two states. The former is a precursor of the true superradiance of many identical atomic systems<sup>28</sup>. Note that this limit can be reached both for identical dots  $\Delta \rightarrow 0$  and for strongly coupled ones  $|V| \gg |\Delta|$ , which makes it important also in the case of typically strongly inhomogeneous QD systems.

The second effect is related to the oscillating term in Eq. (9b). In a general case, it can be expected to have little impact on the secular evolution since the two frequencies  $2\mathcal{E}/\hbar$  and  $E_B/\hbar$  are typically different. However, the biexciton shift depends on the static dipole moment in the dots, hence on the spatial arrangement of the carriers, and can be tuned e.g. by applying an external axial electric field. Therefore, these two frequencies can be tuned to resonance and this term becomes non-negligible. Physically, this means that the transition from the biexciton state to one of the single exciton state has the same energy as the transition from the same single exciton state to the vacuum state. As follows from Eq. (9b), in such case the exciton coherence  $\rho_{0\pm}$  is driven by the biexciton coherence  $\rho_{\pm B}$ , hence coherence can be transferred from the biexciton transition to the exciton transition. In Sec. IV B, we will show that this transfer leads to a considerable modification of the decay of optical coherences in the signal and affects the nonlinear optical spectrum of the system.

For the phonon contribution, we rewrite Eq. (3) in the eigenbasis of the exciton states

$$H_{c-ph} = \sum_{\alpha=\pm} (|\alpha\rangle\langle\alpha| + |B\rangle\langle B|) \sum_{\mathbf{k}} f_{\mathbf{k}}^{(\alpha)} (b_{\mathbf{k}}^{\dagger} + b_{-\mathbf{k}}) + \frac{1}{2} \sin\theta \sum_{\mathbf{k}} F_{\mathbf{k}} (|+\rangle\langle-| + |- \rangle\langle+|), \quad (10)$$

where

$$\begin{aligned} f_{\mathbf{k}}^{(+)} &= \cos^2 \frac{\theta}{2} f_{\mathbf{k}}^{(1)} + \sin^2 \frac{\theta}{2} f_{\mathbf{k}}^{(2)}, \\ f_{\mathbf{k}}^{(-)} &= \sin^2 \frac{\theta}{2} f_{\mathbf{k}}^{(1)} + \cos^2 \frac{\theta}{2} f_{\mathbf{k}}^{(2)}, \end{aligned} \quad (11)$$

and

$$F_{\mathbf{k}} = f_{\mathbf{k}}^{(2)} - f_{\mathbf{k}}^{(1)} = -2if_{\mathbf{k}} \sin \frac{k_z D}{2}.$$

The coexistence of carrier-phonon couplings diagonal and off-diagonal in the carrier eigenstates in this interaction Hamiltonian makes the evolution nontrivial<sup>17</sup>. However,

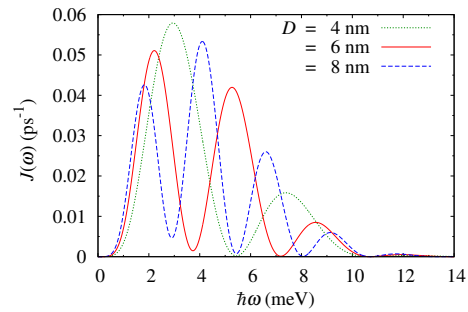


FIG. 1: (Color online) The phonon spectral density for a few values of the inter-dot distance  $D$ .

the diagonal coupling terms in Eq. (10) lead to non-Markovian pure dephasing on a picosecond time scale, while the off-diagonal terms induce transitions, which may be described to a good approximation in the Markov limit and are characterized by time scales of several picoseconds. Using this time scale separation, one can approximately treat the two effects separately for the sake of interpreting the simulation results to be presented in Sec. IV.

The pure dephasing dynamics is due to the lattice response to the ultrafast change of the carrier state<sup>29,30</sup>. As the phonon dynamics depends on the carrier state the lattice gets correlated to the confined carriers and effectively extracts information on the carrier state<sup>31</sup>. This induces dephasing of quantum superpositions of various exciton states, which has been studied from the point of view of the optical response<sup>19</sup> and of the decay of entanglement between the dots<sup>18</sup>. For the present discussion, the essential effect is the dephasing of superpositions between the single exciton eigenstates. Following the approach of Refs. 18,32, one finds the evolution of the corresponding coherence (neglecting the effect of the off-diagonal terms in Eq. (10))

$$\langle +|\rho(t)|- \rangle = \langle +|\rho(0)|- \rangle e^{-h(t)}, \quad (12)$$

where

$$\begin{aligned} h(t) &= 4 \cos^2 \theta \sum_{\mathbf{k}} \left| \frac{f_{\mathbf{k}}}{\omega_{\mathbf{k}}} \right|^2 \sin^2 \frac{k_z D}{2} (1 - \cos \omega_{\mathbf{k}} t) (2n(\omega_{\mathbf{k}}) + 1) \\ &\xrightarrow{t \gg t_{\text{ph}}} 4 \cos^2 \theta \sum_{\mathbf{k}} \left| \frac{f_{\mathbf{k}}}{\omega_{\mathbf{k}}} \right|^2 \sin^2 \frac{k_z D}{2} (2n(\omega_{\mathbf{k}}) + 1) \equiv h_{\infty}, \end{aligned}$$

where  $n(\omega)$  are the phonon occupation numbers and  $t_{\text{ph}}$  is the characteristic time of the phonon-induced initial dephasing which is of the order of a few picoseconds<sup>18</sup>. The factor  $\cos^2 \theta$  reflects the fact that for maximally delocalized eigenstates ( $\theta = \pi/2$ ) the charge distribution is the same for both of them and they cannot be distinguished by the phonon response.

The real transitions governed by the off-diagonal coupling terms in Eq. (10) in many cases take place on a

longer time scale (several picoseconds to tens or hundreds of picoseconds, depending on the amplitude of the coupling) and can be to a good approximation described in terms of the Markovian transition rates  $\gamma_{i \rightarrow j} = 2\pi \sin^2 \theta J(|\omega_{ij}|) |n(\omega_{ij}) + 1|$ , where  $i, j = \pm$ ,  $\omega_{ij} = (E_j - E_i)/\hbar$  and the spectral density is defined as

$$J(\omega) = \sum_{\mathbf{k}} |f_{\mathbf{k}}|^2 \sin^2 \frac{k_z D}{2} \delta(\omega - \omega_{\mathbf{k}}).$$

The spectral density for a few values of the inter-dot spacing  $D$  is plotted in Fig. 1. Apart from the usual cutoff at frequencies larger than  $\bar{l}/c$  due to the restriction on the momentum non-conservation  $\Delta(\hbar k) \lesssim \hbar/\bar{l}$ , where  $\bar{l}$  is the average dot size, it is characterized by the oscillations with the period  $\Delta\omega = 2\pi c/D$  which result from the double dot structure of the system. These oscillations are most pronounced at higher frequencies, where the emission along the  $z$  axis (the strongest confinement direction) dominates, which makes the factor  $\sin^2(k_z D/2)$  most efficient.

The above remarks will provide us with useful guidelines for the interpretation of the simulation results presented in the next section.

#### IV. RESULTS

In this section we present and discuss the results of numerical simulations of the spontaneous emission from double dot system under the influence of phonons. First, in Sec. IV A we study the decay of DQD occupations. Then, in Sec. IV B we describe the effect of coherent transfer of interband dipole moment and study its stability against phonon-induced perturbations. In all the simulations, we assume  $\theta \leq 0$ , hence  $V \leq 0$  and the lower single exciton state  $|-\rangle$  is brighter than the higher state  $|+\rangle$  ( $\Gamma_- \geq \Gamma_+$ ).

##### A. Occupation decay

As discussed in Sec. III, the coupling between the dots leads to the formation of two delocalized eigenstates with different decay rates. For  $V < 0$ , the state  $|+\rangle$  is darker (decays slower) and the state  $|-\rangle$  is brighter (decays faster). This can be seen in Fig. 2(a) (green dashed and blue dotted lines), where we show the evolution of the exciton occupation in the DQD without carrier-phonon coupling (in this case, the evolution depends only on the mixing angle  $\theta$  but not on  $\mathcal{E}$  or the system geometry). For a general initial state, both components are present in a superposition and the decay is not simply exponential, with an average life time in between the two limiting cases. An example of such a situation is shown by the red solid line in Fig. 2(a) for the particularly interesting initial state  $(|1\rangle + |2\rangle)/\sqrt{2}$ , which corresponds to an optical

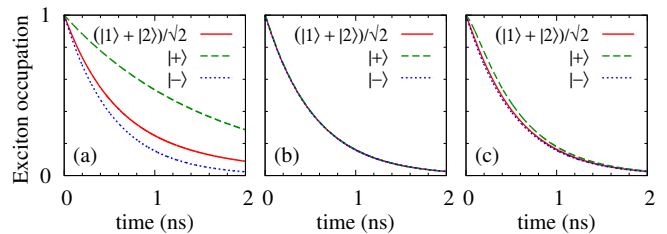


FIG. 2: (Color online) The decay of the exciton occupation for three different initial states as shown for  $D = 6$  nm,  $\theta = -\pi/6$ ,  $T = 4$  K. (a) without carrier-phonon interaction; (b) with phonons, for  $2\mathcal{E} = 1.77$  meV; (c) with phonons, for  $2\mathcal{E} = 3.55$  meV.

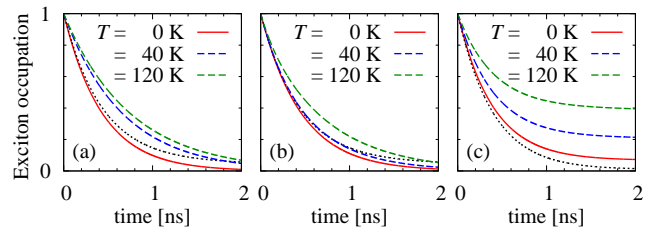


FIG. 3: (Color online) The decay of the exciton occupation for the initial state  $(|1\rangle + |2\rangle)/\sqrt{2}$  for  $D = 6$  nm. (a) dominated by relaxation ( $\theta = -\pi/3$ ) with strong carrier-phonon coupling ( $2\mathcal{E} = 1.77$  meV); (b) as previously but with much weaker phonon effects ( $2\mathcal{E} = 7.1$  meV); (c) dominated by pure dephasing ( $\theta = 0$ ,  $2\mathcal{E} = 0$ ).

excitation by a pulse that resolves the two dots neither spatially nor spectrally.

This kinetics of recombination changes, however, when the carrier-phonon interaction is taken into account, as shown in Fig. 2(b,c). Phonon-induced relaxation redistributes the occupations on a time scale much shorter than the exciton life time, which suppresses the dependence on the initial state. For strong phonon coupling as in Fig. 2(b) (corresponding to the first maximum of the spectral density, see Fig. 1) the resulting radiative decay is almost insensitive to the initial state. The situation is still very similar in the case of energy splitting  $2\mathcal{E}$  corresponding to the first minimum of the spectral density, which yields a much weaker effective coupling, as shown in Fig. 2(c). This shows that the phonon-induced redistribution of occupations dominates the radiative decay over a rather wide range of energy parameters. However, for the values of  $2\mathcal{E}$  around the further minima as well as beyond the effective cut-off at about 10 meV the phonon-related processes become inefficient and the decay becomes similar to that observed in the absence of carrier-phonon coupling.

The important role of phonons in the radiative recombination leads to a strong temperature dependence of the emission process. This effect is shown in Fig. 3, where the exciton occupation decay for the initial optically gen-

erated state  $(|1\rangle + |2\rangle)/\sqrt{2}$  at a few temperatures is plotted for various system parameters. In Fig. 3(a) we choose  $\theta = -\pi/3$  and the value of the energy splitting  $2\mathcal{E}$  close to the first maximum of the spectral density [Fig. 1], which leads to efficient phonon-induced relaxation. The effect of the resulting redistribution of occupations is clearly seen in the dynamics of recombination: with increasing temperature, the occupation of the higher-energy dark state increases at the thermal quasi-equilibrium and the resulting decay becomes slower. Such a change of the recombination rate with temperature can be observed also for higher value of  $2\mathcal{E}$ , corresponding to the deep second minimum of the spectral density. However, in this case the effect is weaker and appears only at higher temperatures, as a considerable occupation of the higher state obviously appears only at  $T \sim \mathcal{E}/k_B$ . In Fig. 3(c) we show that a similar effect of extended life time can appear also due to pure dephasing between the states localized in the two dots<sup>23</sup>. Here, we set  $\theta = 0$ , which excludes occupation redistribution. However, the occupation-conserving pure dephasing effect remains effective and leads to destruction of the coherence between the two single exciton states according to Eq. (12), where, in the present case,  $|+\rangle = |1\rangle$  and  $|-\rangle = |2\rangle$ . Due to this dephasing, the initially bright state is partly turned into a mixture of dark and bright states, in which the probability for the dark state is<sup>23</sup>  $(1 - e^{-h\infty})/2$  and grows with temperature. As the lifetime of the dark state is infinite in this limiting case of parameter values the pure dephasing process effectively leads to a slowed down decay.

The effect of thermal extension of the exciton lifetime is directly reflected in the dynamics of photoluminescence (PL) which may be observed in a time-resolved experiment. We calculate the PL signal by multiplying the occupations of the eigenstates  $|+\rangle$  and  $|-\rangle$  by the corresponding decay rates  $\Gamma_{\pm}$ . In order to account for thermally activated non-radiative processes, we follow Ref. 6 and suppress the values obtained from our simulation by the factor  $\exp(-\Gamma_{nr}t)$ , where  $\Gamma_{nr} = \Gamma_{nr}^{(0)} \exp[-E_a/(k_B T)]$  is the rate of non-radiative exciton decay processes, attributed in Ref. 6 to exciton escape, which are here assumed to affect the two lowest exciton states in the same way. In this model,  $E_a$  is the activation energy for the non-radiative process and  $\Gamma_{nr}^{(0)}$  is its overall strength. The PL decay time is then determined as the time at which the PL intensity (which decays not necessarily exponentially) is reduced by a factor  $1/e$ .

In Fig. 4(a) we plot the decay time of the PL signal from a single DQD structure after initial ultrafast preparation of the state  $(|1\rangle + |2\rangle)/\sqrt{2}$  (in fact, as we discussed above, the initial condition is not very important if the phonon-induced thermalization is fast enough). We choose here a fixed value of  $\Delta = 0.5$  meV,  $E_a = 95$  meV (as estimated in Ref. 6) and  $\Gamma_{nr}^{(0)} = 8.16$  ps<sup>-1</sup> (half of the value in Ref. 6, corresponding to a twice shorter radiative exciton life time assumed in our simulations). Varying the strength of the coupling results in a clear qualitative change of the temperature dependence of the PL decay

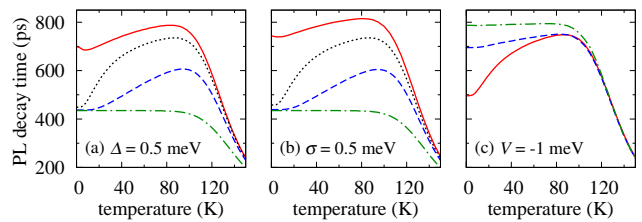


FIG. 4: (Color online) The decay time of the DQD photoluminescence. (a) A single DQD with  $\Delta = 0.5$  meV and  $V = -0.2$  meV (red solid line),  $-1$  meV (black dotted line),  $-3$  meV (blue dashed line), and  $-8$  meV (green dash-dotted line). (b) An ensemble of DQDs with constant values of the coupling  $V$  as in (a), with the average energy mismatch  $\overline{\Delta} = 0$ , and with the standard deviation of  $\Delta$  equal to  $\sigma = 0.5$  meV. (c) An ensemble of DQDs for  $\overline{\Delta} = 0$  and for three values the standard deviation of  $\Delta$ :  $\sigma = 1$  meV (red solid line),  $3$  meV (blue dashed line), and  $10$  meV (green dash-dotted line).

time. The shapes of the curves obtained from the simulations at lower temperatures reflect the rate of the radiative recombination, while at higher temperatures they are dominated by the non-radiative suppression. In general, the thermally increased quasi-equilibrium occupation of the higher, darker state leads to longer PL decay times, reduced at higher temperatures by the non-radiative contribution, which leads to the appearance of a maximum of the decay time. However, for a weak inter-dot coupling (red solid line in Fig. 4(a)), the energy mismatch dominates and the two states are almost equally bright, that is, they have similar radiative decay rates. As a result, even at  $T = 0$ , when only the brighter state is occupied, the decrease of the life time is marginal and the resulting amplitude of the change in the PL decay time is small. This changes when the coupling is stronger (black dotted and blue dashed lines in Fig. 4(a)) so that the ground state has a considerably increased decay rate, which is manifested by a much shorter PL decay time at low temperatures. In a certain range of intermediate values of  $V$  this results in a considerable growth of the PL decay time before the non-radiative effects become important, which leads to the formation of a pronounced maximum. However, for higher coupling strengths the maximum disappears again. Now, the energy splitting between the two states, roughly equal to  $2V$ , is so large that the change of equilibrium occupations is negligible in the temperature range in which the luminescence life time is governed by the radiative decay.

As can be seen In Fig. 4(b), a nearly identical dependence on temperature is obtained for an ensemble of DQDs in which the coupling  $V$  is again assumed fixed and the values of the energy mismatch  $\Delta$  vary across the ensemble according to the Gaussian distribution with the mean value  $\overline{\Delta} = 0$  and a rather small standard deviation  $\sigma = 0.5$  meV. The fact that the ensemble of DQDs is relatively homogeneous in terms of the energy mismatch

$\Delta$  is essential. As we show in Fig. 4(c), if the standard deviation  $\sigma$  becomes larger the shape of the temperature dependence changes considerably. This is due to the fact, that for  $\sigma \gg |V|$  the ensemble is dominated by DQDs with  $\Delta \gg |V|$  for which the collective effects are negligible. Hence, there is no decrease of the PL decay time at low temperatures for such ensembles.

The temperature dependence of the PL decay time obtained from our model is qualitatively similar to that observed in the experiment<sup>6</sup>, where a reduction of the decay time by roughly a factor of two at low temperatures was observed and then a maximum was reached at about 100 K, where the decay time equal to that observed in a reference sample with individual QDs was found. However, as the above discussion shows, such a large amplitude of the variation of the PL decay time is only possible for rather small values of  $V$  (in order to assure a small energy difference required for efficient thermalization). Therefore, our model is unable to quantitatively account for those experimental results obtained in a system containing much more strongly coupled DQDs, in which thermalization of occupations between the bright and dark states could not take place to a sufficient extent in the relevant temperature range. In view of the theory presented here, the origin of the strongly non-monotonic temperature dependence of the PL decay time in such a system remains an interesting issue. Based on our results, we can only conclude that a thermally activated mechanism of breaking the coherent nature of the delocalized exciton state, other than thermalization between the two states included in our model, is needed to account for this behavior.

### B. Transfer of coherence

In this section we study the effect related to the resonance between the biexciton shift  $E_B$  and the energy splitting between the single-exciton states. As discussed in Sec. III, such a resonance affects the decay of interband polarizations in the DQD system, opening the path for a transfer of optical coherence from the biexciton transition to the single exciton transitions, according to Eq. (9b). Here, we first discuss this effect in the absence of phonons. Then, we describe the phonon effects on this coherence transfer. Finally, we show that this dynamics of interband coherences is manifested by a line narrowing in nonlinear absorption spectra.

In Fig. 5, we present the evolution of the interband coherences (optical polarizations) for a single DQD in the situation when the single-exciton transition  $|-\rangle \rightarrow |0\rangle$  is energetically close to the biexciton transition  $|B\rangle \rightarrow |-\rangle$ , without taking into account the carrier-phonon interaction. We plot the evolution of the excitonic polarization  $P_X = |\rho_{0-}|$ , the biexcitonic polarization  $P_{XX} = |\rho_{-B}|$  and the total polarization in the spectral vicinity of the two transitions, defined as  $P_{\text{total}} = |\rho_{0-} + \rho_{-B}|$ . Figs. 5(a-c) show the dynamics for uncoupled dots ( $V = 0$ ) at exact

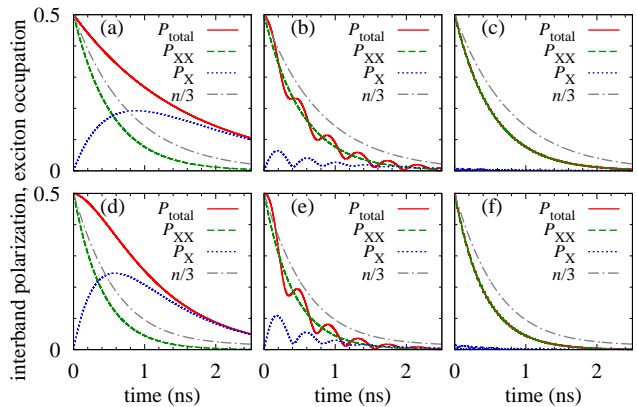


FIG. 5: (Color online) The evolution of single-exciton, biexciton and total optical coherence for a DQD with  $2\mathcal{E} = 3$  meV in the absence of interaction with phonons. (a-c) Uncoupled dots with  $E_B = -3$  meV,  $-3.01$  meV, and  $-3.1$  meV, respectively. (d-f) Coupled dots with  $\theta = -\pi/3$  and with the same values of  $E_B$  as in (d-f), respectively. In all the panels the red solid line shows the total polarization, the green dashed line represents the biexciton polarization and the blue dotted line shows the single-exciton polarization. The evolution of the average exciton occupation (scaled down by a factor of 3 to fit to the polarization amplitudes) is shown with gray dash-dotted lines for comparison.

resonance,  $E_B = -2\Delta = -3$  meV and for two slightly off-resonant situations corresponding to  $|E_B| - 2\Delta = 0.01$  meV and  $0.1$  meV. The initial state of the DQD is chosen to be  $(|-\rangle + |B\rangle)/\sqrt{2}$ . In all the three cases, the biexciton polarization (green dashed line) decays exactly in the same way (with the rate  $\Gamma_0 + \Gamma_-/2 = 3\Gamma_0/2$  in this case). However, at resonance, its decay is accompanied by the appearance of a relatively long-living exciton polarization (blue dotted line). Hence, the decay time of the total coherence (red solid line) is considerably extended. This effect is present only in a narrow energy range around the resonance. Already for a detuning of  $0.01$  meV, the transfer of coherence to the single-exciton polarization is much smaller and the decay of the total polarization is only modulated by small oscillations. Finally, at still larger detunings from the resonance, the coherence transfer vanishes completely and no increase of the polarization decay time is observed. As can be seen in Figs. 5(d-f), the evolution is very similar for coupled dots. Here all the time scales are slightly shorter since the involved single-exciton state is partly superradiant. It should be noted that the strong variation of the polarization decay time at this particular resonance does not affect the evolution of exciton occupations, as represented by the gray dash-dotted lines which show identical decay independent of the detuning.

In Fig. 6, we plot the evolution of the same optical polarizations as in Fig. 5 but taking into account the carrier-phonon coupling. In all the cases, the value of  $E_B$  is set at resonance (including compensation for phonon-induced

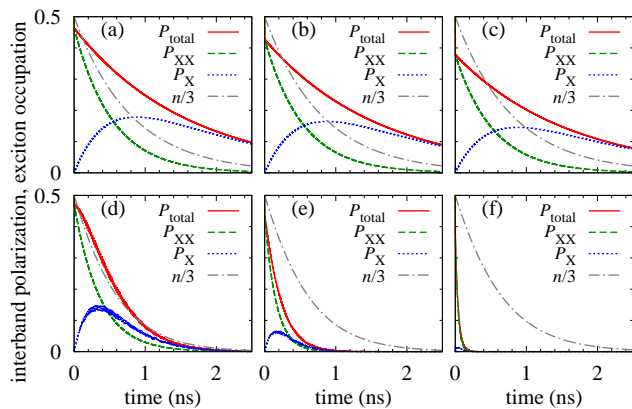


FIG. 6: (Color online) The evolution of single-exciton, biexciton and total optical coherence for a DQD with  $2\mathcal{E} = 3$  meV with the carrier-phonon coupling taken into account. The value of  $E_B$  is taken at resonance. (a-c) Uncoupled dots at  $T = 0$ , 10 K and 20 K, respectively. (d-f) Coupled dots with  $\theta = -\pi/3$  at the same three temperatures. Line coding as in Fig. 5.

energy shifts which are below 0.1 meV). Figs. 6(a-c) correspond to uncoupled dots ( $V = 0$ ) at the temperature  $T = 0$  K (a), 10 K (b), and 20 K (c). In this case, the evolution of polarizations is weakly affected by phonons due to the suppression of the phonon-induced real transitions between the two eigenstates. The only effect is the fast initial dephasing of the coherence<sup>29</sup> which increases with temperature. In Figs. 6(d-f), we present the evolution of a DQD system with coupled dots ( $\theta = -\pi/3$ , which corresponds to  $V \approx 1.3$  meV and  $\Delta \approx 0.75$  meV). Here we see that the lifetime of the polarization is shortened to some extent already at  $T = 0$  and becomes very short at  $T = 20$  K. The amplitude of the single-exciton polarization induced by the polarization transfer also decreases with temperature. The effect of pure dephasing is visible also here but it affects the evolution only over a very short period and leads to a small almost instantaneous initial reduction of the polarization. The strong temperature dependence observed at longer times is due to real phonon-induced transitions between the single exciton eigenstates which is allowed in the case of coupled dots and is accompanied by a decay of coherences between the single exciton states involved in these phonon-induced transitions and the other two states (vacuum and biexciton). Since our initial state involves only the lower-energy single exciton state the phonon scattering within the single exciton subspace induces the Markovian dephasing of the interband coherences with a rate which critically depends on the Bose occupation factor at the phonon frequency corresponding to the transition to the higher state,  $n_B(2\mathcal{E}/\hbar)$ . The major phonon-induced effect is therefore thermally activated. At higher temperatures it reduces the lifetime of the polarizations from the usual time scales of radiative recombination to the values typical for phonon-related processes, that is, from almost

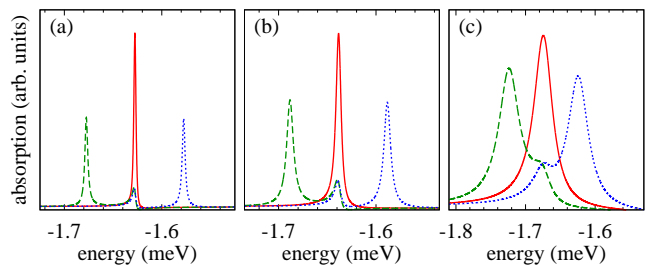


FIG. 7: (Color online) The pump-probe absorption spectra (see text) at  $T = 4$  K (a), 10 K (b), and 20 K (c). Each plot shows three lines corresponding to exact resonance (red solid lines) and to a detuning of 0.05 meV and  $-0.05$  meV from the resonance (blue dotted and green dashed lines, respectively). Here  $2\mathcal{E} = 3$  meV,  $\theta = -\pi/3$ .

a nanosecond to several picoseconds.

While the analysis of the evolution of the individual contributions to the polarization gives insight in the mechanisms underlying the system kinetics, these quantities are not directly accessed in an experiment. In order to study features related to the biexciton coherences one usually resorts to nonlinear spectroscopy techniques<sup>2,13,33</sup>. For instance, the effects of dipole couplings between the dots have been thoroughly studied theoretically for the differential absorption measured in a pump-probe experiment<sup>13</sup>. Tracing the phonon effects on such spectra on the same level of exactness would require including carrier-phonon coupling in the full model of Ref. 13 which would go far beyond the scope of this paper. Here, we only present a simplified model of a particular pump-probe experiment in which the extended life times of the optical coherences are manifested in the absorption spectra in the most clear way.

Let us consider a pump-probe experiment in which the spectrally resolved lowest-order response of a single pair of coupled dots to a probe pulse is studied after a strong pump pulse (beyond the usual second order in the pump amplitude). The two pulses are spectrally broad enough to excite all the relevant exciton and biexciton transitions in an identical way. The delay time between the pulses is long enough for the occupations of the two single-exciton states to equilibrate but much shorter than the radiative life time. We assume that the area of the pump pulse  $\alpha_{\text{pump}}$  is such that  $\sin^2(\alpha_{\text{pump}}/2) = 1/\{2 - \tanh[\mathcal{E}/(k_B T)]\}$ . This choice strongly suppresses the gain line corresponding to the emission from the ground exciton state leaving the biexciton absorption line as the only feature in the relevant spectral range. We then calculate the probe absorption spectrum as the imaginary part of the Fourier transform of the total polarization obtained from the simulations with the initial state corresponding to an instantaneous excitation by the probe from the thermalized state prepared by the pump (in the linear order in the probe pulse area).



The spectra obtained in this way, in the area around the transition energy from the lowest exciton state, are shown in Fig. 7. Here the energy is shown with respect to the average fundamental transition energy  $E = (\epsilon_1 + \epsilon_2)/2$ . Each plot contains three spectra: one at resonance (red solid line) and two detuned by  $\pm 0.05$  meV. Each off-resonant spectrum contains the absorption line corresponding to the exciton-biexciton transition and a weak feature at the exciton-ground state transition energy. The essential effect is the narrowing of the absorption line at the resonance, which corresponds to the extended life time of the coherent polarization due to the coherence transfer to single-exciton polarization, as discussed above. This effect is quite strong at low temperatures but becomes less pronounced when the temperature increases and the line widths become dominated by phonon-related effects.

## V. CONCLUSION

We have studied theoretically the kinetics of radiative recombination of excitons confined in systems consisting of two coupled quantum dots in the presence of carrier-phonon coupling. In general terms, this corresponds to spontaneous emission from non-identical coupled emitters undergoing an additional, possibly non-Markovian dephasing. We have shown that coupling to phonons strongly affects the dynamics of spontaneous emission by inducing transitions between the bright and dark states of the double-dot structure as well as by pure dephasing processes at short time scales. Both these phonon-related effects lead to strong temperature dependence of the carrier lifetime. We have shown that in the case of

a binding ground state (negative coupling, typical e.g. for tunneling), the carrier lifetime increases with growing temperature. For certain values of system parameters and in the presence of thermally activated non-radiative exciton decay processes, this can lead to a non-monotonic dependence of the exciton lifetime.

We have also studied the process of resonant coherence transfer between the biexciton and exciton transitions and the effect of phonons on the kinetics of this process. We have shown that this effect can lead to considerable extension of the life time of coherent interband polarization in the double dot system, which is stable against phonon-induced decoherence in a relatively wide temperature range. We have presented a simplified model of a spectrally resolved pump-probe experiment which shows that the coherence transfer and the resulting extension of the polarization life time manifests itself by line narrowing in the nonlinear absorption spectrum of the system.

Our results show that carrier-phonon interaction can qualitatively modify the optical response of double dot systems. Phonon-related effects turn out to play a much more important role in these systems than they do for individual dots. Our modeling can shed some light on the existing experimental results but also allowed us to predict new features that can be sought for in future experiments.

## Acknowledgments

This work was partly supported by the Foundation for Polish Science under the TEAM programme, co-financed by the European Regional Development Fund.

---

\* Electronic address: Pawel.Machnikowski@pwr.wroc.pl

<sup>1</sup> J. E. Rolon and S. E. Ulloa, Phys. Rev. B **82**, 115307 (2010).

<sup>2</sup> T. Unold, K. Mueller, C. Lienau, T. Elsaesser, and A. D. Wieck, Phys. Rev. Lett. **94**, 137404 (2005).

<sup>3</sup> O. Gywat, G. Burkard, and D. Loss, Phys. Rev. B **65**, 205329 (2002).

<sup>4</sup> M. Goryca, T. Kazimierzczuk, M. Nawrocki, A. Golnik, J. A. Gaj, P. Kossacki, P. Wojnar, and G. Karczewski, Phys. Rev. Lett. **103**, 087401 (2009).

<sup>5</sup> P. Borri, W. Langbein, U. Woggon, M. Schwab, M. Bayer, S. Fafard, Z. Wasilewski, and P. Hawrylak, Phys. Rev. Lett. **91**, 267401 (2003).

<sup>6</sup> C. Bardot, M. Schwab, M. Bayer, S. Fafard, Z. Wasilewski, and P. Hawrylak, Phys. Rev. B **72**, 035314 (2005).

<sup>7</sup> B. D. Gerardot, S. Strauf, M. J. A. de Dood, A. M. Bychkov, A. Badolato, K. Hennessy, E. L. Hu, D. Bouwmeester, and P. M. Petroff, Phys. Rev. Lett. **95**, 137403 (2005).

<sup>8</sup> G. W. Bryant, Phys. Rev. B **47**, 1683 (1993).

<sup>9</sup> B. Szafran, S. Bednarek, and J. Adamowski, Phys. Rev. B **64**, 125301 (2001).

<sup>10</sup> W. Jaskólski, M. Zieliński, G. W. Bryant and J. Aizpurua, Phys. Rev. B **74**, 195339 (2006).

<sup>11</sup> B. Szafran, Acta Phys. Polon. A **114**, 1013 (2008).

<sup>12</sup> A. Sitek and P. Machnikowski, Phys. Rev. B **75**, 035328 (2007).

<sup>13</sup> J. Danckwerts, K. J. Ahn, J. Förstner, and A. Knorr, Phys. Rev. B **73**, 165318 (2006).

<sup>14</sup> A. O. Govorov, Phys. Rev. B **68**, 075315 (2003).

<sup>15</sup> M. Richter, K. J. Ahn, A. Knorr, A. Schliwa, D. Bimberg, M. E.-A. Madjet, and T. Renger, Phys. Stat. Sol. (b) **243**, 2302 (2006).

<sup>16</sup> E. Rozbicki and P. Machnikowski, Phys. Rev. Lett. **100**, 027401 (2008).

<sup>17</sup> A. Grodecka-Grad and J. Förstner, Phys. Rev. B **81**, 115305 (2010).

<sup>18</sup> K. Roszak and P. Machnikowski, Phys. Rev. A **73**, 022313 (2006).

<sup>19</sup> J. Huneke, A. Krügel, T. Kuhn, A. Vagov, and V. M. Axt, Phys. Rev. B **78**, 085316 (2008).

<sup>20</sup> E. A. Muljarov, T. Takagahara, and R. Zimmermann, Phys. Rev. Lett. **95**, 177405 (2005).

<sup>21</sup> A. Sitek and P. Machnikowski, Phys. Rev. B **80**, 115319

- (2009).
- <sup>22</sup> A. Sitek and P. Machnikowski, Phys. Rev. B **80**, 115301 (2009).
- <sup>23</sup> P. Machnikowski, J. Phys: Conf. Ser. **193**, 012136 (2009).
- <sup>24</sup> P. Machnikowski, K. Roszak, and A. Sitek, Acta Phys. Polon. A **116**, 818 (2009).
- <sup>25</sup> C. Hermannstädter, G. J. Beirne, M. Witzany, M. Heldmaier, J. Peng, G. Bester, L. Wang, A. Rastelli, O. G. Schmidt, and P. Michler, Phys. Rev. B **82**, 085309 (2010).
- <sup>26</sup> B. Szafran, T. Chwiej, F. M. Peeters, S. Bednarek, J. Adamowski, and B. Partoens, Phys. Rev. B **71**, 205316 (2005).
- <sup>27</sup> H.-P. Breuer and F. Petruccione, *The Theory of Open Quantum Systems* (Oxford University Press, Oxford, 2002).
- <sup>28</sup> M. Gross and S. Haroche, Phys. Rep. **93**, 301 (1982).
- <sup>29</sup> B. Krummheuer, V. M. Axt, and T. Kuhn, Phys. Rev. B **65**, 195313 (2002).
- <sup>30</sup> L. Jacak, P. Machnikowski, J. Krasnyj, and P. Zoller, Eur. Phys. J. D **22**, 319 (2003).
- <sup>31</sup> K. Roszak and P. Machnikowski, Phys. Lett. A **351**, 251 (2006).
- <sup>32</sup> K. Roszak, P. Machnikowski, and L. Jacak, Phys. Stat. Sol. (b) **243**, 2261 (2006).
- <sup>33</sup> E. G. Kavousanaki, O. Roslyak, and S. Mukamel, Phys. Rev. B **79**, 155324 (2009).